High thermoelectric power factor in Fe-substituted Mo3Sb7

Christophe Candolfi, Bertrand Lenoir, Anne Dauscher, Bernard Malaman, Emmanuel Guilmeau, Jiří Hejtmánek, Janusz Tobola

Applied Physics Letters

High thermoelectric power factor in Fe-substituted Mo_3Sb_7

Cite as: Appl. Phys. Lett. **96**, 262103 (2010); https://doi.org/10.1063/1.3457920
Submitted: 16 March 2010 • Accepted: 26 May 2010 • Published Online: 28 June 2010

C. Candolfi, B. Lenoir, A. Dauscher, et al.

High thermoelectric power factor in Fe-substituted Mo_3Sb_7

C. Candolfi,[1,a)] B. Lenoir,[1] A. Dauscher,[1] B. Malaman,[1] E. Guilmeau,[2] J. Hejtmanek,[3] and J. Tobola[4]

[1]*Institut Jean Lamour, Ecole Nationale Supérieure des Mines de Nancy, UMR 7198 CNRS-Nancy Université-UPVM, Parc de Saurupt, 54042 Nancy Cedex, France*

[2]*CRISMAT-ENSICAEN, UMR 6508, 6 Bd Maréchal Juin, 14050, Caen Cedex, France*

[3]*Institute of Physics, Academy of Sciences of the Czech Republic, Cukrovarnicka 10, CZ-162 53, Praha 6, Czech Republic*

[4]*Faculty of Physics and Applied Computer Science, AGH University of Science and Technology, 30-059 Krakow, Poland*

(Received 16 March 2010; accepted 26 May 2010; published online 28 June 2010)

Thermoelectric properties of the $Mo_{2.57}Fe_{0.43}Sb_7$ compound, a ternary derivative of Mo_3Sb_7, are reported from 2 up to 1000 K. Even though Fe substitution keeps low electrical resistivity values, high thermopower values are achieved at high temperatures. Electronic band structure calculations show that the high thermopower observed arises from the beneficial influence of iron *d*-states contribution to the density of states at the Fermi level. A high power factor similar to those of the best state-of-the-art thermoelectric materials emerges which, coupled with magnetic excitations that help to keep very low thermal conductivity values, leads to a dimensionless thermoelectric figure of merit of 0.55 at 1000 K. © *2010 American Institute of Physics*. [doi:10.1063/1.3457920]

As the search for prospective materials for thermoelectric applications intensified in the past decade, complex intermetallic systems such as skutterudites, clathrates, half-Heusler alloys, or Zintl phases have emerged as prime candidates.[1] These exciting discoveries were driven by some basic guidelines, based on solid state physics considerations, provided in the 50s and extended in the early 90s by several theoretical ideas.[2,3] Such empirical criterions stand for the desirable features a material should possess to deserve great attention from researchers in thermoelectricity. The essence of these fundamental requirements can be quantitatively captured by the dimensionless figure of merit *ZT* defined, at a temperature *T*, by $ZT=\alpha^2T/\rho\lambda=PT/\lambda$ where α is the Seebeck coefficient or thermopower, ρ the electrical resistivity, λ the total thermal conductivity, and *P* the power factor.[2] To achieve high *ZT* values require materials exhibiting low electrical resistivity encountered in metallic crystals as well as thermal properties obtained in glass-like systems.

Recently, sharp hybridization-induced structures and resonant levels near the Fermi level have appeared as efficient ways to enhance the thermopower and thus to achieve high *ZT* values. Such prominent features in the electronic band structure have been experimentally underlined in PbTe doped with Tl and in the metallic $CoSi_{1-x}Ge_x$ compounds as mechanisms from which enhanced thermoelectric properties may appear.[4,5]

In this letter, we show that the substitution of Mo by Fe in Mo_3Sb_7 provides an additional example of such engineering of the density of states (DOS) near the Fermi level. The beneficial influence of Fe leads to a high power factor and thus, to a substantially higher dimensionless thermoelectric figure of merit compared to that of Mo_3Sb_7.

Detailed descriptions of the metallurgical route used to synthesize a polycrystalline sample of $Mo_{2.57}Fe_{0.43}Sb_7$, of the chemical and structural characterizations techniques employed, of the transport properties measurements in the low and high temperature range and of the theoretical method used to calculate the electronic band structure can be found elsewhere.[6] X-ray diffraction and electron probe microanalysis have shown that this sample contains a small amount of Fe-rich secondary phases. The actual composition was determined to be $x=0.43$ which constitutes the solubility limit of Fe in Mo_3Sb_7. In the next paragraphs, we shall always refer to the actual composition.

Figures 1(a) and 1(b) show the temperature dependence of the electrical resistivity and the Seebeck coefficient of $Mo_{2.57}Fe_{0.43}Sb_7$ and of Mo_3Sb_7 for comparison purposes. Across the entire temperature range investigated, the temperature coefficient of the electrical resistivity is positive $(d\rho/dT)$ indicative of a metallic-like behavior for both compounds. Upon alloying, the electrical resistivity still assumes low values which increase from 1.8 $\mu\Omega$ m in Mo_3Sb_7 to 2.2 $\mu\Omega$ m in $Mo_{2.57}Fe_{0.43}Sb_7$ at 300 K. Nonetheless, for both samples, the measured values are at least one order of magnitude higher than those usually displayed by pure me-

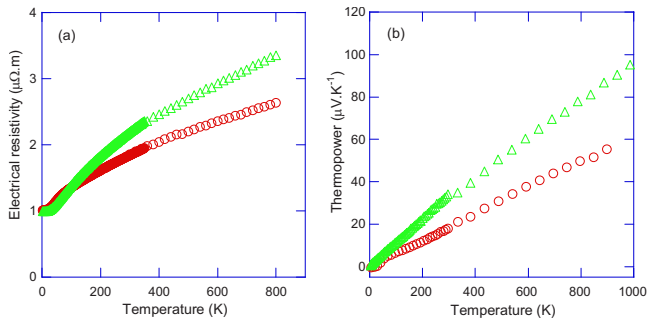

FIG. 1. (Color online) Temperature dependences of the (a) electrical resistivity and (b) Seebeck coefficient of the Mo_3Sb_7 (○) and $Mo_{2.57}Fe_{0.43}Sb_7$ (△) compounds.

a)Authors to whom correspondence should be addressed. Electronic addresses: candolfi@mines.inpl-nancy.fr and candolfi@cpfs.mpg.de. Present address: Max-Planck-Insitut für Chemische Physik fester Stoffe, Nöthnitzer Str. 40, 01187 Dresden, Germany.

tallic elements or alloys.[7] Hall effect experiments performed at room temperature have shown that the Fe substituted sample exhibits a *p*-type conduction, as the parent compound does. The carrier concentration, p, inferred from the simple relation $p=1/R_He$ where R_H is the Hall coefficient and e the elementary charge, is only slightly lowered from 8.5×10^{21} carriers cm^{-3} in Mo_3Sb_7 to 7.1×10^{21} carriers cm^{-3} in $Mo_{2.57}Fe_{0.43}Sb_7$.

If on a more fundamental level, such a high carrier concentration should imply low thermopower values, a very different picture emerges from the experimental data [Fig. 1(b)]. The $Mo_{2.57}Fe_{0.43}Sb_7$ compound exhibits high positive thermopower values reaching ~100 $\mu V\,K^{-1}$ at 1000 K. Both the temperature dependence of the Seebeck coefficient and the magnitude of α linearly increase with temperatures up to 1000 K revealing a purely diffusive nature. High thermopower values coupled with low electrical resistivity values give rise to a high power factor $P=\alpha^2/\rho\approx26$ $\mu W\,cm^{-1}\,K^{-1}$ at 1000 K for $Mo_{2.57}Fe_{0.43}Sb_7$, comparable with those of the best state-of-the-art thermoelectric materials.[2]

A comprehensive analysis of the thermopower is usually based on the Mott's formula suggesting that any variation in α arises as a direct consequence of modifications of the electronic band structure near the Fermi level. This relation can be mathematically written as

$$\frac{\alpha}{T}=-\frac{\pi^2k_B^2}{3e}\left[\frac{\partial\ln N(E)}{\partial E}\right]_{E=E_F}, \tag{1}$$

where k_B is the Boltzmann constant, E the energy, and $N(E)$ the DOS.[8] As evidenced by Eq. (1), α is proportional to the slope of the DOS in the vicinity of the Fermi level E_F. Thus, to investigate the underlying mechanisms responsible for the observed high thermopower values required to calculate the electronic band structure of the material, which in turn requires a precise knowledge of the crystallographic parameters, i.e., the lattice parameter and the atomic coordinates. In the present case, the partial substitution of Mo by Fe raises an additional difficulty related to the knowledge of the exact position of the iron atoms in the Mo_3Sb_7 cubic structure. It has been previously suggested that a low iron content might be inserted into the cubic voids formed by the antimony atoms of the Mo_3Sb_7 structure.[9–11] Whether or not iron atoms can be localized in this alternative position constitutes an issue that must be settled before undertaking such calculations. To definitively clarify this point, we carried out Mössbauer effect experiments enabling to probe the local atomic environment, i.e., the charge distribution and magnetic field surrounding the Fe nucleus. To avoid any parasitic signal coming from the small amount of the Fe-rich phases, this study was performed on a $Mo_{2.65}Fe_{0.35}Sb_7$ sample exhibiting any detectable secondary phase neither by x-ray and neutron diffraction nor by chemical analyses. In the present case, the situation appears favorable since only two different crystallographic sites are involved, i.e., the alternative site of cubic symmetry and the molybdenum site located at the center of an antimony antiprism that exhibits a noncubic symmetry. The recorded Mössbauer spectrum, shown in Fig. 2, is characterized by a well-defined quadrupole splitting typified by two symmetric peaks. The full width at half maximum of the peaks closely corresponds to that observed for pure iron crystal. This clearly demonstrates that a unique population of

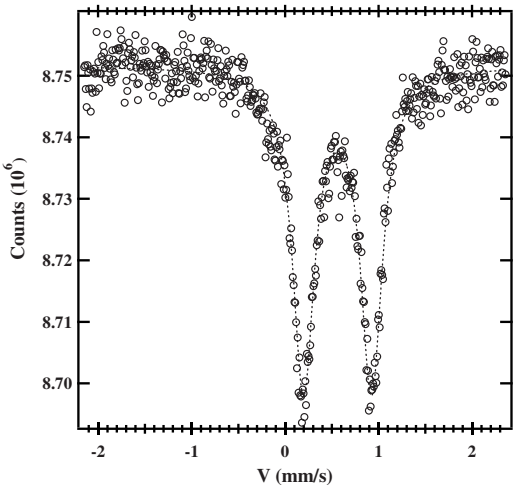

FIG. 2. ^{57}Fe Mössbauer spectrum of $Mo_{2.65}Fe_{0.35}Sb_7$ recorded at 300 K. The dotted curve stands for the best fit to the data using Lorentzian-shaped functions. The values of the derived hyperfine parameters are 0.56 and 0.73 mm s^{-1} for the isomer shift and the quadrupole splitting, respectively.

iron atoms inserted in the crystalline lattice of Mo_3Sb_7 can be held responsible for the observed data, further supporting the absence of secondary phases in this sample. Since the quadrupole splitting can be only distinguished when iron atoms are located on a noncubic symmetry site, this analysis unequivocally shows that iron only substitutes molybdenum.

Taking into account this essential crystallographic information, band structure calculations were carried out. Figure 3 shows a magnification of the top of the valence bands of Mo_3Sb_7 superimposed with those of the Fe substituted sample. As expected for a *p*-type material, the valence bands host the Fermi level. Our calculations demonstrate that the Fermi level is slightly shifted toward the band gap in $Mo_{2.57}Fe_{0.43}Sb_7$ consistent with additional electrons delivered by Fe atoms. However, contrarily to the rigid-band behavior of the electronic band structure observed for the $Mo_3Sb_{7-x}Te_x$ and $Mo_{3-x}Ru_xSb_7$ compounds against Te and Ru content,[6] this result reveals a breakdown of a rigid-like picture in $Mo_{3-x}Fe_xSb_7$ further corroborated by the evolution of the dispersion curves (not shown). The Fermi level is positioned at 340 and 270 meV from the valence band edge at $T=0$ K in Mo_3Sb_7 and $Mo_{2.57}Fe_{0.43}Sb_7$, respectively.

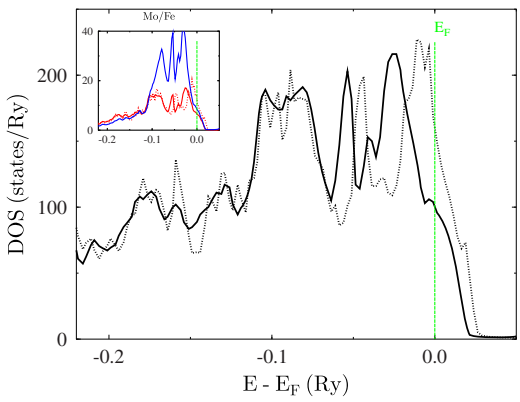

FIG. 3. (Color online) DOS near the Fermi level of the Mo_3Sb_7 (dotted line) and $Mo_{2.57}Fe_{0.43}Sb_7$ (solid line) compounds. The Fermi energy, E_F, has been arbitrarily positioned at zero energy (vertical line). The inset displays the site-dependent densities of states of Mo (lower solid curve) and Fe (upper solid curve) atoms.

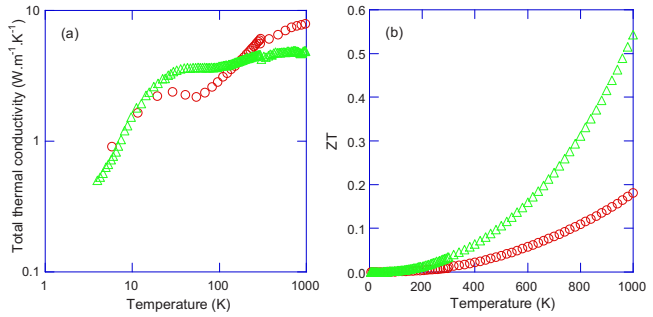

FIG. 4. (Color online) Temperature dependences of the (a) total thermal conductivity and (b) ZT of the Mo_3Sb_7 (○) and $Mo_{2.57}Fe_{0.43}Sb_7$ (△) compounds.

These values result in reduced Fermi levels $\eta=E_F/k_BT$ of ~14 and 11 in Mo_3Sb_7 and $Mo_{2.57}Fe_{0.43}Sb_7$ at 300 K, respectively, which largely exceed the value that delineates the highly degenerate from the partially degenerate regime ($\eta=4$). This result thus suggests that the Fe-substituted sample is still metallic in nature.

The additional iron d-states contribution to $N(E_F)$ results in an increased slope near the Fermi level compared to Mo_3Sb_7. Using the Mott's formula [Eq. (1)], the high experimental thermopower values of $Mo_{2.57}Fe_{0.43}Sb_7$ mainly originate from this feature. A quantitative estimation of the DOS slope near the Fermi level, α/T, derived assuming a single band model with energy independent relaxation time yields $\alpha/T \sim 0.11$ μV K^{-2} for $Mo_{2.57}Fe_{0.43}Sb_7$, in excellent agreement with the experimental slope of ~0.10 μV K^{-2}. One may object that the observed increase in the thermopower values is a natural consequence of the decrease in the carrier concentration upon alloying with Fe. Detailed investigations of the transport properties of the ternary $Mo_3Sb_{7-x}Te_x$ and $Mo_{3-x}Ru_xSb_7$ systems have shown that in both case increasing x results in a decrease in the carrier concentration.[6] However, for a similar carrier concentration, the observed enhancement of the thermopower values is less pronounced in these two above-mentioned systems.[6] These results clearly indicate that the sharp DOS slope induced by the partial substitution of Mo by Fe is the central aspect leading to higher thermopower values and hence, to high power factors.

The temperature dependence of the total thermal conductivity is depicted in Fig. 4(a). It is worth mentioning that the lower thermal conductivity values exhibited by Mo_3Sb_7 in the 50–100 K temperature range is mainly a consequence of the magnetic interactions and the spin gap formation as already shown in $Mo_3Sb_{7-x}Te_x$ and $Mo_{3-x}Ru_xSb_7$.[6,12] Given the low electrical resistivity values, the thermal conductivity is very small in the whole temperature range and attains 5 W m^{-1} K^{-1} at 1000 K. Beyond this value, the overall temperature dependences of both Mo_3Sb_7 and $Mo_{2.57}Fe_{0.43}Sb_7$ are appealing in the sense that they do not resemble to the conventional behavior that characterizes a dielectric crystal. The distinction might be disclosed in the low-dimensional magnetism exhibited by Mo_3Sb_7 and related to antiferromagnetically coupled molybdenum dimers leading to a spin gap formation at $T^*=53$ K.[6,12] Specifically, the exotic behavior of the thermal conductivity has been proposed to originate from a strong interplay between phonons and the magnetic interactions associated to the Mo–Mo dimers resulting in strongly depressed lattice thermal conductivity up to 1000 K.[6] Can such magnetic properties also account for the observed behavior in the Fe substituted sample? Though apparently the spin gap, as a direct indicator of complex magnetic framework, does no longer open when Mo is substituted by Fe, transport as well as magnetic properties experiments carried out on the $Mo_3Sb_{7-x}Te_x$ and $Mo_{3-x}Fe_xSb_7$ systems have evidently shown that these magnetic interactions still act as an efficient phonon scattering mechanism for samples exhibiting a carrier concentration above $\sim 3\times 10^{21}$ cm^{-3}.[6] Consequently, a strong phonons-spins scattering combined with a complex crystalline structure might explain why the total thermal conductivity of $Mo_{2.57}Fe_{0.43}Sb_7$ remains so low even at 1000 K.

The beneficial impact of iron on the DOS slope in the vicinity of the Fermi level coupled with magnetic excitations and complex crystal structure constitute three favorable circumstances from which a high dimensionless thermoelectric figure of merit ZT of ~0.55 can emerge at 1000 K [Fig. 4(b)]. Not only does this result provide significant information regarding the possibility to optimize the thermoelectric properties of a metallic system by inducing sharp DOS features near the Fermi level through substitutions but it also emphasizes the potential of this material for technological applications beyond the thermoelectricity borders. The ability to easily produce homogeneous samples with the desired Fe concentration (up to ~0.45) and the perfectly linear temperature dependence of the thermopower in a wide temperature range make this system a prospective candidate to become a Seebeck coefficient standard reference material.

The authors warmly thank C. Bellouard for magnetotransport measurements. C.C. greatly thanks M. Amiet and P. Maigné and financial support of DGA (Délégation Générale pour l'Armement, Ministry of Defense, France) and the European Network of Excellence CMA (Complex Metallic Alloys). B.L. acknowledges the support of the "Region Lorraine" through the CPER project. J.H. acknowledges the financial support of the Czech Science Foundation (Grant No. 203/09/1036). J.T. acknowledges the partial support of the Polish Ministry of Science and Higher Education (Grant No. 44/N-COST/2007/0).

[1] G. J. Snyder and E. S. Toberer, Nature Mater. **7**, 105 (2008), and references therein.
[2] H. J. Goldsmid, *Thermoelectric Refrigeration* (Temple, London, 1964).
[3] D. M. Rowe, *CRC Handbook of Thermoelectrics: Macro to Nano* (CRC, Boca Raton, 2005).
[4] J. P. Heremans, V. Jovovic, E. S. Toberer, A. Saramat, K. Kurosaki, A. Charoenphakdee, S. Yamanaka, and G. J. Snyder, Science **321**, 554 (2008).
[5] E. Skoug, C. Zhou, Y. Pei, and D. T. Morelli, Appl. Phys. Lett. **94**, 022115 (2009).
[6] C. Candolfi, B. Lenoir, A. Dauscher, J. Hejtmanek, and J. Tobola, Phys. Rev. B **80**, 155127 (2009), and references therein.
[7] *Metals: Electronic Transport Phenomena*, edited by K.-H. Hellwege and O. Madelung, Landolt-Börnstein, New Series, Group III, Vol. 15a (Springer, Berlin, 1982).
[8] N. F. Mott and E. A. Davis, *Electronic Processes in Non-Crystalline Materials* (Clarendon, Oxford, 1971).
[9] E. Dashjav, A. Szczepenowska, and H. Kleinke, J. Mater. Chem. **12**, 345 (2002).
[10] U. Häussermann, M. Elding-Ponten, C. Svensson, and S. Lidin, Chem.-Eur. J. **4**, 1007 (1998).
[11] H. Xu, K. M. Kleinke, T. Holgate, H. Zhang, Z. Su, T. M. Tritt, and H. Kleinke, J. Appl. Phys. **105**, 053703 (2009).
[12] V. H. Tran, W. Miiller, and Z. Bukowski, Phys. Rev. Lett. **100**, 137004 (2008).